International Journal of Mechanical, Industrial and Aerospace Sciences
ISSN: 2517-9950
Vol:7, No:11, 2013

A Hybrid Differential Transform Approach for Laser Heating of a Double-Layered Thin Film

Cheng-Ying Lo

***Abstract*—**This paper adopted the hybrid differential transform approach for studying heat transfer problems in a gold/chromium thin film with an ultra-short-pulsed laser beam projecting on the gold side. The physical system, formulated based on the hyperbolic two-step heat transfer model, covers three characteristics: (i) coupling effects between the electron/lattice systems, (ii) thermal wave propagation in metals, and (iii) radiation effects along the interface. The differential transform method is used to transfer the governing equations in the time domain into the spectrum equations, which is further discretized in the space domain by the finite difference method. The results, obtained through a recursive process, show that the electron temperature in the gold film can rise up to several thousand degrees before its electron/lattice systems reach equilibrium at only several hundred degrees. The electron and lattice temperatures in the chromium film are much lower than those in the gold film.

***Keywords*—**Differential transform, hyperbolic heat transfer, thin film, ultrashort-pulsed laser.

I. Introduction

ULTRA short laser pulse has become a popular laser manufacturing technique to avoid the thermal damage due to the diffusion of laser energy in work pieces and to improve manufacturing quality [1]. The ultra-short pulsed laser will induce high temperature gradient, up to thousands of degrees in Kevin temperature, within a very short duration of time, ranging from sub-picoseconds to femtoseconds, during manufacturing processes. The traditional Fourier heat transfer model, which assumes the infinite speed of thermal waves, cannot be applied to analyze the heat transfer phenomena of engineering applications with high-power for a short-duration [2]. Cattaneo [3] and Vernotte [4] proposed the hyperbolic heat transfer model to account for the effects of thermal waves travelling at a finite speed.

Because the heat capacity of the electron system is much smaller than that of the lattice system in metals, the high thermal unbalance will occur after the short duration of laser excitation. Energy flux between electron and lattice will continue after laser duration. Anisimov, Kapeliovich and Perelman [5] proposed the two-step model to model the energy absorption process in the laser manufacturing process, which assumes that laser energy is absorbed first by the electron system and then flows into the lattice system through the coupling thermal effects between the two systems and the rise of the lattice temperature follows. Qiu and Tien [6] integrated the thermal wave effects into the two-step model of the electron system. Their work studied heat transfer mechanisms during ultrashort laser heating process from a microscopic point of view. Chen and Beraun [7] modified Qiu and Tien's model to include the thermal wave effects in the lattice system. Jiang and Tsai [8] are able to determine electron heat capacity, electron relaxation time, electron conductivity, reflectivity, and absorption coefficient using the full-run quantum treatment. Several numerical works have been done in studying laser heating of a single layer thin film based on the hyperbolic two-step model [7], [9], [10].

It is quite often that microelectronic devices are constructed with multilayer thin films. Refection and refraction of thermal waves may occur at the interface between dissimilar materials. Ho, Kuo and Jiaung [11] studied the propagation of an ultrashort pulsed energy across the solid interface of dissimilar material layers using the lattice Boltzmann method. Lor and Chu [12] considered the hyperbolic heat conduction problem in the film and substrate composites. Barron and Dai [13] studied the 3D parabolic heat transfer in a double-layered thin film using the hybrid finite-element- finite-difference method. Wang, Dai and Hewavitharana [14] further included the effects of thermal deformation in a double-layered thin film exposed to ultrashort pulsed lasers. The speed of thermal waves is considered infinite in the parabolic heat transfer model.

When dealing with the hyperbolic heat transfer problem numerically, it often encounters nonphysical numerical oscillation near the thermal wave front. Many numerical procedures have been proposed to eliminate those difficulties such as MacCormack's predictor-corrector scheme [15], flux differencing scheme [16], [17], and the total variation diminishing (TVD) scheme [18], [19]. The differential transform method, which is a function transformation technique based on Taylor's series, is developed mainly to solve initial value problems [20]. Recently, the differential transform method has successfully been applied to many engineering problems. Peng and Chen [21] use the differential transform method to the energy transfer induced by laser irradiation in the solid with an energy source modeled based upon Beer's law. Chiba [22] analyzes the one-dimensional steady temperature field and thermal stresses in an annular disk of variable thickness with a temperature-dependent heat transfer coefficient. The present study intends to integrate the differential transformation method with the finite difference method to solve heat transfer problems in a double-layered thin film exposed to an ultrashort pulsed laser based on the double hyperbolic two-step model. The differential transform method is used to transfer the governing equations in the time domain

C. Y. Lo is with the Department of Aeronautical Engineering, National Formosa University, Huwei Yunlin 632, Taiwan ROC (e-mail: cylo@nfu.edu.tw).

into the spectrum equations, which is further discretized in the space domain by the finite difference method. The distribution of the electron and lattice temperatures is solved.

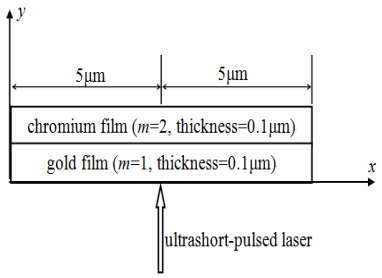

Fig. 1 Physical system of a double-layered thin film exposed to an ultrashort-pulsed laser

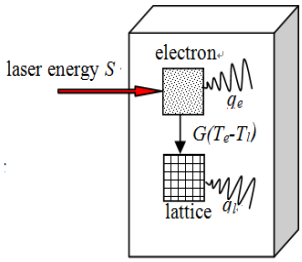

Fig. 2 The hyperbolic two-step heat transfer model of laser heating

II. Mathematical Model

Consider a double-layered thin film exposed to an ultrashort -pulsed laser as shown in Fig. 1. The upper layer is made of chromium and the bottom layer is made of gold. Thermo-physical properties of gold and chromium are listed in Table I. Both layers have a thickness of 0.1μm and a length of 10μm. An ultrashort pulsed laser is applied at the gold side at the center point from below. When an ultrashort pulsed laser interacts with a metal thin film, the laser energy is first absorbed by free electrons and then transfers to the lattice system. The energy also propagates away at a finite speed from the interaction location through the thermal diffusion in the electron system and lattice system. The process is characterized as the hyperbolic two-step heat transfer model as shown in Fig. 2. Assume that the major laser energy transfers across the gold/chromium interface mainly through the thermal radiation due to the temperature difference between the gold/chromium electron temperatures. No energy flows across the interface between the gold/chromium lattice systems. The complete physical system covers three characteristics: (i) coupling effects between the electron/lattice systems, (ii) thermal wave propagation in metals, and (iii) radiation effects along the interface. Let superscript (m) be the material code, m =1 refers to the gold layer and m=2 refers to the chromium layer. Subscripts e and l refer to the electron system and the lattice system respectively. The Gaussian laser heat source function and governing equations, accounting for laser energy absorption, thermal coupling between electron/lattice, and thermal waves, are given as [14]

TABLE I
Thermophysical Properties

Parameters	Gold	Chromium
C_{e0}	2.1×10^{-14} J/μm^{3}K	5.8×10^{-14} J/μm^{3}K
C_l	2.5×10^{-12} J/μm^{3}K	3.3×10^{-12} J/μm^{3}K
G	2.6×10^{10} W/μm^{3}K	42×10^{10} W/μm^{3}K
k_0	315×10^{-6} W/μmK	94×10^{-6} W/μmK
k_l	315×10^{-6} W/μmK	94×10^{-6} W/μmK
ρ	19300×10^{-18} kg/μm^3	7190×10^{-18} kg/μm^3
τ_e	0.04ps	0.04ps
τ_l	0.8ps	0.8ps

Gaussian laser heat source:

$$S(x,y,t)=0.94J\frac{1-R}{t_p y_s}\exp\left[-\frac{y}{y_s}-\frac{(x-x_0)^2}{r_s^2}-2.77\left(\frac{t-2t_p}{t_p}\right)^2\right] \quad (1)$$

Electron energy equations:

$$\begin{aligned} C_e^{(m)}\left(T_e^{(m)}\right)\frac{\partial T_e^{(m)}}{\partial t}&=-\frac{\partial q_e^{x(m)}}{\partial x}-\frac{\partial q_e^{y(m)}}{\partial y}-G\left(T_e^{(m)}-T_l^{(m)}\right)+S \\ \tau_e^{(m)}\frac{\partial q_e^{x(m)}}{\partial t}+q_e^{x(m)}&=-k_e^{(m)}\frac{\partial T_e^{(m)}}{\partial x} \\ \tau_e^{(m)}\frac{\partial q_e^{y(m)}}{\partial t}+q_e^{y(m)}&=-k_e^{(m)}\frac{\partial T_e^{(m)}}{\partial y} \end{aligned} \quad (2)$$

Lattice energy equations:

$$\begin{aligned} C_l^{(m)}\left(\frac{\partial T_l^{(m)}}{\partial t}\right)&=-\frac{\partial q_l^{x(m)}}{\partial x}-\frac{\partial q_l^{y(m)}}{\partial y}+G\left(T_e^{(m)}-T_l^{(m)}\right) \\ \tau_l^{(m)}\frac{\partial q_l^{x(m)}}{\partial t}+q_l^{x(m)}&=-k_l^{(m)}\frac{\partial T_l^{(m)}}{\partial x} \\ \tau_l^{(m)}\frac{\partial q_l^{y(m)}}{\partial t}+q_l^{y(m)}&=-k_l^{(m)}\frac{\partial T_l^{(m)}}{\partial y} \end{aligned} \quad (3)$$

Here, t is the time, S is the energy absorption rate, J is the laser fluence, R is the surface reflectivity, t_p is the laser pulse duration, y_s is the optical penetration depth, r_s is the spatial profile parameter, and x_0 is the laser acting position. T is the temperature, k is the thermal conductivity, G is the electron-lattice coupling factor, C is the heat capacity, τ is the relaxation times. q^x and q^y are the heat fluxes in the x and y directions respectively. It is assumed that the electron heat capacity varies linearly with the electron temperature for both gold and chromium, $C_e=C_{e0}(T_e/T_0)$, and the electron thermal conductivity depends on both the electron and lattice temperature, $k_e=k_0(T_e/T_l)$, where C_{e0}, k_0, T_0 are the reference values of electron heat capacity, electron thermal conductivity and temperature, respectively. The nonlinear interfacial radiation condition is given as [23]

$$-k_e^{(1)}\frac{\partial T_e^{(1)}}{\partial y}=-k_e^{(2)}\frac{\partial T_e^{(2)}}{\partial y}=\kappa_B\left[\left(T_e^{(1)}\right)^4-\left(T_e^{(2)}\right)^4\right] \quad (4)$$

Here, $\kappa_B = 5.669\times10^{-8}$ W/μm^{3}K^2 is Boltzman's constant. The electron temperature and lattice temperature may be discontinuous across the gold/chromium interface. Assume that the electron/lattice system of the double-layered thin film is at equilibrium at T_0 and there is no energy flux across the surfaces boundary in a very short of time duration. The initial conditions and the boundary conditions are

$$\begin{aligned} &T_e^{(m)} = T_l^{(m)} = T_0 \quad \text{for} \quad m = 1,2 \quad \text{at} \quad t = 0 \\ &\frac{\partial T_e^{(m)}}{\partial \vec{n}} = \frac{\partial T_e^{(m)}}{\partial \vec{n}} = 0 \quad \text{for} \quad m = 1,2 \quad \text{along four edges} \end{aligned} \tag{5}$$

III. Numerical Differential Transform Procedures

The definition and operation of the differential transform method used in the present study are outlined briefly. Assuming that $f(t)$ is an analytic function, the differential transform of $f(t)$ at t=0 is defined based on the Taylor's expansion series as

$$F(k) = T[f(t)] = \frac{H^k}{k!}\left[\frac{d^k f(t)}{dt^k}\right]_{t=0} \qquad k = 1,2,3,\cdots \tag{6}$$

H is the time span. $F(k)$ is the spectrum function of $f(t)$ in the spectrum domain. The inverse differential transform procedure is defined as the infinite sum. However, practically, the original function $f(t)$ is usually approximated by the n-th partial sum of power series as

$$f(t) = \sum_{k=0}^{n}\left(\frac{t}{H}\right)^k F(k) \tag{7}$$

Usually, the capital letter represents the differential transforms of the functions denoted by the corresponding lowercase letters, i.e., $F(k)$ is the spectrum function of $f(k)$. Let $h(t)=f(t)g(t)$, $z(t)=f(t)/g(t)$, then the spectrum functions of $h(t)$ and $z(t)$ are defined as

$$H(k) = T[h(t)] = \sum_{l=0}^{k} F(l)G(k-l) \tag{8}$$

$$Z(k) = T[z(t)] = \frac{F(k) - \sum_{l=0}^{k-1}\left[F(l)\Big/G(l)\right]G(k-l)}{G(0)} \tag{9}$$

The numerical procedures for applying the hybrid differential transform / finite difference method to solve present heat transfer problem include three major steps: (i) The governing equations, initial conditions and boundary conditions in the time domain are transformed into the spectrum equations, which are given in the recursive formulae, in the spectrum domain. (ii) The resulting spectrum equations are discretized by the finite difference method. (iii) The starting spectrum functions, n=1, are determined by the initial conditions. The successive spectrum functions, n>1, are further calculated from the recursive formulae and the associated boundary conditions. (iv) The original function is calculated by the finite partial sum of the spectrum function in the inverse transform procedure.

To avoid confusion, if the original functions are given in the capitalized form, their spectrum functions are expressed by adding ˜ on the top of the original capital letters in the following paragraphs. After applying the differential transform to the governing equations in (2) and (3) with respect to the time, the resulting spectrum equations in the recursive form are

Recursive electron energy spectrum equations:

$$\begin{aligned} &\frac{C_{e0}^{(m)}}{T_{e0}}\frac{(k+1)}{H}\tilde{T}_e^{(m)0}\tilde{T}_e^{(m)k+1} = -\frac{\partial Q_e^{x(m)k}}{\partial x} - \frac{Q_e^{y(m)k}}{\partial y} \\ &- G\left(\tilde{T}_e^{(m)k} - \tilde{T}_l^{(m)k}\right) + \tilde{S}^k - \frac{C_{e0}^{(m)}}{T_{e0}}\sum_{l=0}^{k-1}\frac{(k+1)}{H}\tilde{T}_e^{(m)l}\tilde{T}_e^{(m)k-l+1} \\ &\tau_e^{(m)}\frac{(k+1)}{H}Q_e^{x(m)k+1} = -k_e^{(m)}\frac{\partial \tilde{T}_e^{(m)k}}{\partial x} - Q_e^{x(m)k} \\ &\tau_e^{(m)}\frac{(k+1)}{H}Q_e^{y(m)k+1} = -k_e^{(m)}\frac{\partial \tilde{T}_e^{(m)k}}{\partial y} - Q_e^{y(m)k} \end{aligned} \tag{10}$$

Recursive lattice energy spectrum equations:

$$\begin{aligned} &C_l^{(m)}\tilde{T}_l^{(m)k} = -\frac{\partial Q_l^{x(m)k}}{\partial x} - \frac{Q_l^{y(m)k}}{\partial y} + G\left(\tilde{T}_e^{(m)k} - \tilde{T}_l^{(m)k}\right) \\ &\tau_l^{(m)}\frac{(k+1)}{H}Q_l^{x(m)k+1} = -k_l^{(m)}\frac{\partial \tilde{T}_l^{(m)k}}{\partial x} - Q_l^{x(m)k} \\ &\tau_l^{(m)}\frac{(k+1)}{H}Q_l^{y(m)k+1} = -k_l^{(m)}\frac{\partial \tilde{T}_l^{(m)k}}{\partial y} - Q_l^{y(m)k} \end{aligned} \tag{11}$$

The interfacial radiation condition is rewritten as

$$-k_e^{(1)}\frac{\partial \tilde{T}_e^{(1)k}}{\partial y} = \kappa_B\left[\begin{array}{l} \sum_{l=0}^{k}\left(\sum_{p=0}^{l}\tilde{T}_e^{(1)p}\tilde{T}_e^{(1)l-p}\right)\left(\sum_{p=0}^{k-l}\tilde{T}_e^{(1)p}\tilde{T}_e^{(1)k-l-p}\right) \\ -\sum_{l=0}^{k}\left(\sum_{p=0}^{l}\tilde{T}_e^{(2)p}\tilde{T}_e^{(2)l-p}\right)\left(\sum_{p=0}^{k-l}\tilde{T}_e^{(2)p}\tilde{T}_e^{(2)k-l-p}\right) \end{array}\right] \tag{12}$$

The initial and boundary condition along the four edges are rewritten as

$$\begin{aligned} &\tilde{T}_e^{(m)}(1) = \tilde{T}_l^{(m)}(1) = T_0 \ \text{ for } m = 1,2 \\ &\frac{\partial \tilde{T}_e^{(m)}(k)}{\partial \vec{n}} = \frac{\partial \tilde{T}_l^{(m)}(k)}{\partial \vec{n}} = 0 \text{ for } m = 1,2 \ k = 1,2,\cdots \end{aligned} \tag{13}$$

Equations (10)-(13) are further discretized by the traditional finite difference method, which is described here. The spectrum functions for all k>1 are calculated sequentially from the recursive equations and the boundary conditions, once the starting spectrum functions, k=1, are directly given by the initial conditions. Usually, the time span H is assigned to be one time increment Δt , which should carefully selected based on numerical accuracy and computation time. The numerical procedure is repeatedly calculated at each time step, in which the starting spectrum functions at each time step are replaced by the spectrum functions at the end of the previous time step.

IV. Numerical Examples

In the following numerical study, the laser heat source in (1) has the following manufacturing parameters: R=0.93, t_p=0.1ps, y_s=15.3×10^{-3}μm, r_s=1μm, initial temperature T_0=300K and the laser fluence J is set at three different levels, J=500, 1000, and 2000J/m^2. After several convergent tests, the time span is set to be H=0.001ps and the space domain is divided into 100×100 grid nodes. Fig. 3 shows the electron/lattice temperatures right at the laser acting location at x=5μm and y=0μm on the gold surface. The laser heat source reaches its maximum at t=0.2ps. The electron temperature rises rapidly to about 6700K for J=2000J/m^2 because the laser energy is absorbed by free electrons first and drops gradually to about 1800K at t=20ps. At the same time, the lattice temperature gradually increases to about 900K by absorbing heat flux from the electrons. Even after the laser pulse is removed, the lattice temperature is on the rise because the higher electron temperature. When J reduces to J=500J/m^2, the maximum electron temperature reduces to about 3500K and the electron/lattice systems almost reach the equilibrium temperature at about 400K. Fig. 4 shows the electron/lattice temperatures at x=5μm and y=0.1μm in the chromium film. The heat energy has to transfer across the interface by radiation, which is more significant at high temperature. The electron/lattice temperatures are much lower than in the gold film. The maximum electron temperature is about 349K for J=2000J/m^2. Very small lattice temperature rise is observed in the chromium film, about 2K even with J=2000J/m^2. The electron/lattice systems also reach the equilibrium state at about t=1.2ps, which is much faster than in the gold film. Since the thermal waves take time to travel from the gold surface to the interface, the maximum electron temperature occurs slightly later at t=0.27ps.

The distribution of the electron/lattice temperatures are demonstrated by the case with J=1000J/m^2. Figs. 5 and 6 show the electron temperature and the lattice temperature in the x-direction on the gold surface (y=0μm) respectively. Figs. 7 and 8 show the electron temperature and the lattice temperature of the chromium film in the x-direction at the interface (y=0.1μm) respectively. The major region under the effects of laser heating is within 3μm<x<7μm. The temperature outside the region shows no significant increase. Since the laser source is at its maximum strength at t=0.2ps, the electron temperature drops from largest values at t=0.2ps to smaller values at t=20ps. On the contrary, the lattice temperature increases from the initial temperature. The trend is quite consistent on the gold surface and along the chromium interface except that there is a great temperature difference between them.

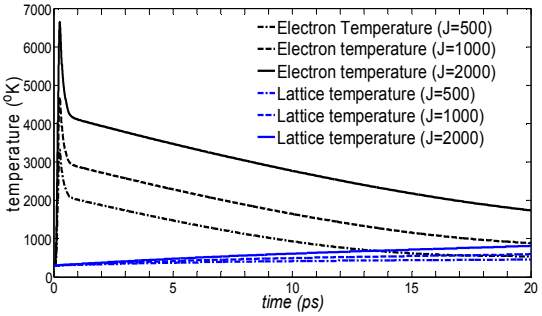

Fig. 3 Gold's temperatures at x=5μm,y=0μm

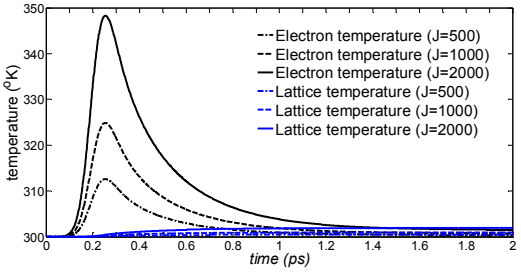

Fig. 4 Chromium's temperatures at x=5μm,y=0.1μm

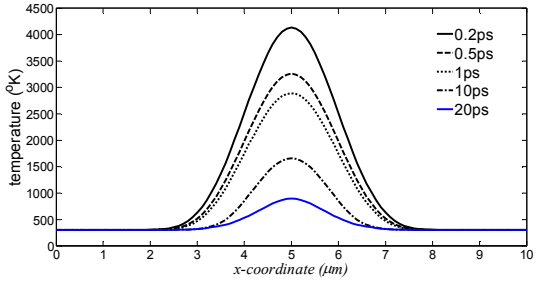

Fig. 5 Gold's electron temperature at y=0μm (J=100J/m^{2}K)

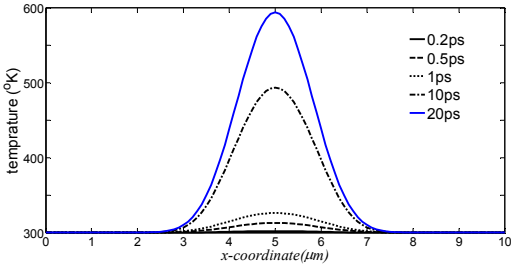

Fig. 6 Gold's lattice temperature at y=0.1μm (J=100J/m^{2}K)

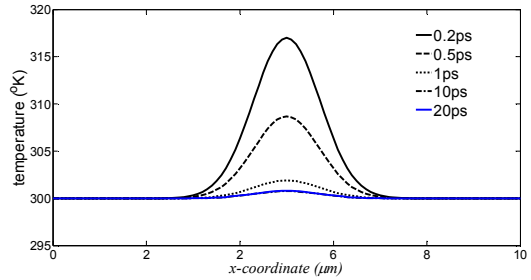

Fig. 7 Chromium's electron temperature at y=0.1μm (J=100J/m^{2}K)

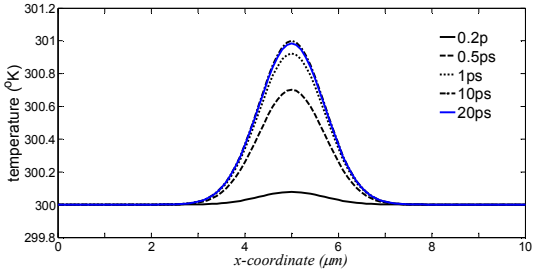

Fig. 8 Chromium's lattice temperature at y=0.1μm (J=100J/m^{2}K)

Figs. 9 and 10 show the electron/lattice temperatures through the thickness at x=5μm at t=0.2,0.5,1,10,20ps. The phenomena caused by thermal waves are obviously observed in the gold film. At t=0.2ps, the electron temperature reaches its maximum on the gold surface at about 4100K. It drops to about 900K at t=20ps. However, at the interface of the gold side, the electron temperature remains low at about 400K at t=0.2ps since the laser energy takes time to propagate toward the interface. The electron temperature at the interface increases to about 2900K at t=1ps while the electron temperature decreases on the gold surface. After t=10ps, the electron temperature through the thickness in the gold film drops uniformly to about 900K at t=20ps. At t=0.2ps, the lattice temperature on the gold surface is slightly higher than at the gold interface. As the laser heat source decreases and the thermal waves propagate toward the interface, the gold's lattice temperature at the interface becomes higher than that on the gold surface. It is noted that at t=10ps, the gold's lattice temperature at the interface is about 100K higher than on the surface. At t=20ps, it increases up to 1200K, which is higher than the gold's electron temperature at the interface. It is due to the reflection of the thermal waves at the interface since there is no energy flux across the interface in the lattice system. The laser energy flows across the interface only through the electron system. The thermal damage may take place at the interface because the thermal reflection wave. The temperature difference between the gold layer and chromium layer is significant; the electron/lattice temperature near the interfacial region is closely examined further.

Figs. 11-16 examine the electron/lattice temperature through the thickness in the region near the interface (0.08μm<y< 0.12μm) with different laser fluence levels at different time (t=0.2, 0.5, 1ps). At t=0.2ps, the temperature differences in the electron temperature at the interface are very small, about 250K for J=2000J/m^{2}K as shown in Fig. 11. There is a very small amount of energy flux across the interface by radiation. Though the temperature increase in the lattice system at the interface is very small at t=0.2ps (less than 0.2 K), it is noted that in Fig. 12 the chromium's lattice temperature is higher than the gold's lattice temperature at the interface. Because the temperature difference between the electron/lattice system is rather small at this moment for both gold and chromium, the larger coupling coefficient G of chromium means that the energy is more easily to transfer from the electron system into the lattice system. At the later time, the temperature difference between the electron /lattice system in the gold film becomes much higher than in the chromium film as shown in Figs. 13 and 14. The energy flowing into in the lattice system of the gold film increases because of the large temperature difference. It causes the higher lattice temperature in the gold film. Figs. 15 and 16 show that the electron temperature difference between gold and chromium increases from about 1700K for J=500J/m^{2}K to 3900K for J=2000J/m^{2}K at t=1ps. However, the maximum lattice temperature differences are below 25K for all J values. The results also indicate that the chromium film is only slightly affected under the laser heating process in the present study.

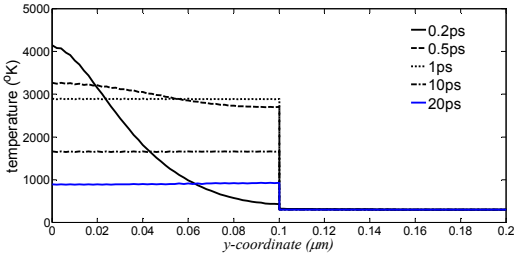

Fig. 9 Electron temperature through thickness at x=5μm (J=100J/m^{2}K)

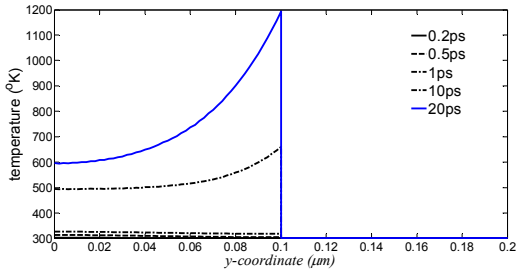

Fig. 10 Lattice temperature through thickness at x=5μm (J=100J/m^{2}K)

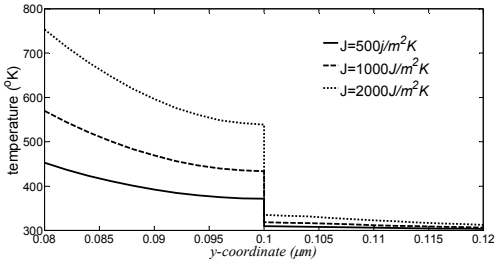

Fig. 11 Electron temperature through thickness at x=5μm, t=0.2ps

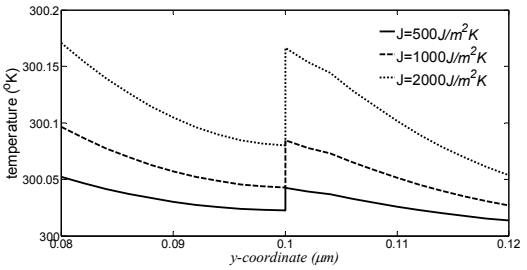

Fig. 12 Lattice temperature through thickness at x=5μm, t=0.2ps

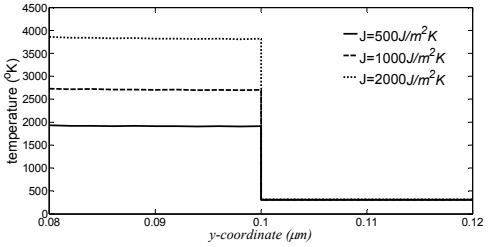

Fig. 13 Electron temperature through thickness at x=5μm, t=0.5ps

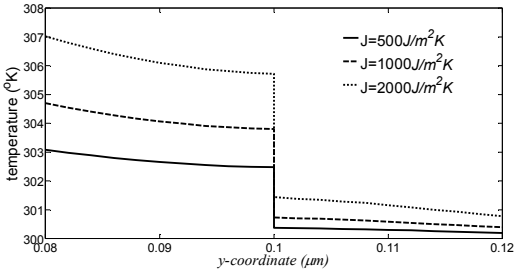

Fig. 14 Lattice temperature through thickness at x=5μm, t=0.5ps

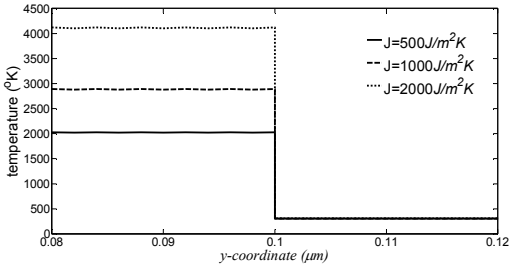

Fig. 15 Electron temperature through thickness at x=5μm, t=1ps

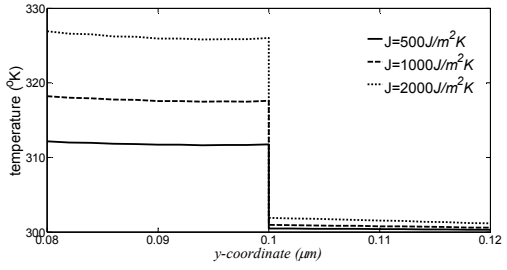

Fig. 16 Lattice temperature through thickness at x=5μm, t=1ps

V. Conclusion

A hybrid differential transform method can be used to solve the hyperbolic two-step heat transfer problems in laser heating of a double-layered thin film. It is efficient and can be easily implemented. The results show the lattice temperature may increase dramatically due to the reflection of thermal at the interface. The interfacial conditions have a significant effect on the present case and should be examined carefully.

Acknowledgment

This project has been fully supported by the National Science Council, Taiwan, ROC, under Grant NSC 100-2221-E-150 - 020

References

[1] M. D. Shirk, and P. A. Molian, "A review of ultrashort pulsed laser ablation of materials," *J. Laser Appl.*, vol. 10, pp. 18–28, 1998.
[2] T. T. Lam, "A unified solution of several heat conduction model," *Int. J. Heat Mass Transfe*r, vol. 56, pp. 653–666, 2013.
[3] C. Cattaneo, "Sur une forme de l'equation de la chaleur elinant le paradoxe d'une propagation instantance," Comptes Rendus, vol. 247, pp. 431-433, 1958.
[4] M. P. Vernotte, "Les paradoxes de la theorie continue de l'equation de la chaleur," Comptes Rendus, vol. 246, pp. 3154-3155, 1958.
[5] S. I. Anisimov, B. L. Kapeliovich, and T. L. Perelman, "Electron Emission from Metal Surfaces Exposed to Ultrashort Laser Pulses," *Sov. Phys. JETP* 39, pp. 375–377, 1974.
[6] T. Q. Qiu, and C. L. Tien, "Heat Transfer Mechanisms during Short-Pulse Laser Heating of Metals," *J. Heat Transfer*, vol. 115, pp. 835-841, 1993.
[7] J. K. Chen, J. E. Beraun, "Numerical study of ultrashort laser pulse interactions with metal films," *Numer. Heat Transfer Part A*, vol. 40, pp. 1–20, 2001.
[8] L. Jiang, and H. L. Tsai, "Improved Two-Temperature Model and Its Application in Ultrashort Laser Heating of Mental Films," *J. Heat Transfer*, vol. 127, pp. 1167-1173, 2005..
[9] M. Al-Odat, M. A. Al-Nimr, and M. Hamdan, "Thermal Stability of Superconductors under The Effect of a Two-Dimensional Hyperbolic Heat Conduction Model," *Int. J. Numer. Meth. Heat Fluid Flow*, vol. 12, pp. 173–177, 2002.
[10] M. A. Al-Nimr, O. M. Haddad, and V.S. Arpaci, "Thermal Behavior of Metal Films—A Hyperbolic Two-Step Model," *Heat Mass Transfer*, vol. 35, pp. 459–464, 1999.
[11] J. R. Ho, C. P. Kuo, and W. S. Jiaung, "Study of heat transfer in multilayered structure within the framework of dual-phase-lag heat conduction model using lattice Boltzmann method," Int. J. Heat Mass Transfer, Vol. 46, pp. 55-69, 2003.
[12] W. B. Lor, and H. S. Chu, " Hyperbolic heat conduction in thin-film high Tc superconductors with interface thermal resistance," *Cryogenics*, vol. 39, pp. 739-750, 1999.
[13] B. R. Barron, and W. Z. Dai, "A hybrid FE-FD scheme for solving parabolic two-step micro heat transport equations in an irregulary shaped three-dimensional double-layered thin film ," *Numer. Heat Transfer Part B*, vol. 49, pp. 437-465, 2006.
[14] H. J. Wang, W. Z. Dai, and L. G. Hewavitharana, "A finite difference method for studying thermal deformation in a double-layered thin film with imperfect interfacial contact exposed to ultrashort pulsed lasers," Int. J. Thermal Sci., vol. 47, pp. 7-24, 2008.
[15] D. E. Glass, M. N. Ozisik, D. S. McRae, and B. Vick, "On the numerical solution of hyperbolic heat conduction," *Numer. Heat Transfer*, vol. 8, pp. 497–504, 1985.
[16] W. K. Yeung, and T. T. Lam, "A numerical scheme for non-Fourier heat conduction, Part I: One-dimensional problem formulation and applications ," *Numer. Heat Transfer B*, vol. 33, pp. 215–233, 1998.
[17] T. T. Lam, and W. K. Yeung, "A numerical scheme for non-Fourier heat conduction, Part II: Two-dimensional problem formulation and verification,," *Numer. Heat Transfer B*, vol. 41, pp. 543-564, 2002
[18] H. Q. Yang, "Solution of two-dimensional hyperbolic heat conduction by high-resolution numerical methods," *Numer. Heat Transfer A*, vol. 21, pp. 333–349, 1992.

[19] W. Shen, and S. Han, "An explicit TVD scheme for hyperbolic heat conduction in complex geometry, " *Numer. Heat Transfer B*, vol. 41, pp. 565–590, 2002.
[20] C. L. Chen, and Y. C. Liu, "Solution of two-boundary-value-problems using the differential transform method," *J. of Optim. Theory and Appl.*, vol.99, pp. 23-35, 1998.
[21] H. S. Peng, and C. L. Chen, "Application of hybrid differential transformation and finite difference method on the laser heating problem," *Numerical Heat Transfer: Part A* , vol. 59, p28-42, 2011.
[22] R. Chiba, "Application of differential transform method to thermoelastic problem for annular disks of variable thickness with temperature-dependent parameters," Int. J. Thermophysics, vol. 33, pp. 363-380, 2012.
[23] W. B. Lor, and H. S. Chu, "Effect of interface thermal resistance on heat transfer in a composite medium using the thermal wave model," Int. J. Heat Mass Transfer, vol. 43, pp.653–663, 2000.